



ELSEVIER

Available online at www.sciencedirect.com

SCIENCE @ DIRECT®

PALAEO

Palaeogeography, Palaeoclimatology, Palaeoecology 226 (2005) 205–213

www.elsevier.com/locate/palaeo

Dry climate near the Western Pacific Warm Pool: Pleistocene caliches of the Nansha Islands, South China Sea

Shou-Yeh Gong^{a,*}, Horng-Sheng Mii^b, Kuo-Yen Wei^c, Chorng-Sherng Horng^d,
Chen-Feng You^e, Fu-Wen Huang^f, Wen-Rong Chi^f, Tzen-Fu Yui^d, Pei-Keng Torng^f,
Shieu-Tsann Huang^f, Shih-Wei Wang^a, Jong-Chang Wu^f, Kenn-Ming Yang^f

^aDepartment of Geology, National Museum of Natural Science, Taichung, Taiwan

^bDepartment of Earth Sciences, National Taiwan Normal University, Taipei, Taiwan

^cDepartment of Geosciences, National Taiwan University, Taipei, Taiwan

^dInstitute of Earth Sciences, Academia Sinica, Taipei, Taiwan

^eDepartment of Earth Sciences, The National Cheng-Kung University, Tainan, Taiwan

^fExploration and Development Research Institute, Chinese Petroleum Corporate, Miaoli, Taiwan

Received 8 September 2004; received in revised form 12 May 2005; accepted 23 May 2005

Abstract

The Nansha (Spratly) Islands are located in the middle of the South China Sea (at about 10°N) near the northwestern margin of the Western Pacific Warm Pool (WPWP). A borehole was drilled at an atoll at Nansha, and cores were taken. The upper 165.4 m of the borehole consists entirely of limestone of reef facies and lagoon facies, which had been influenced by extensive meteoric diagenesis. Petrographic and geochemical studies have identified at least four subaerial exposure surfaces (SES) in the Pleistocene carbonate sequence. These SES are thought to have resulted from global sea-level changes and characterized by caliche formation.

When developed in limestone, caliches typically form in areas where annual precipitation ranges from 500 mm up to about 1200 mm, compared with 1800–2200 mm of annual rainfall of the present-day Nansha Islands. The Nansha caliche therefore indicates the existence of several dry climate episodes during Pleistocene sea-level lowstands. Lower rainfall and higher evaporation during such dry conditions may explain the higher sea-surface salinities reported elsewhere in the South China Sea. The Nansha caliche may also indicate reduced extent of the WPWP and southerly shift of the Intertropical Convergence Zone during major sea-level lowstands.

© 2005 Elsevier B.V. All rights reserved.

Keywords: Caliche; Palaeoclimate; Sea-level changes; Nansha Islands; South China Sea

1. Introduction

Scientists are divided as to the climates of western Pacific tropical seas during glacial periods. Determin-

* Corresponding author. Fax: +886 4 23222653.

E-mail address: gng@mail.nmns.edu.tw (S.-Y. Gong).

ing how cold it was has been the focal point of various investigations (see the review by De Deckker et al., 2002; Lea et al., 2002). In recent years, other aspects of the palaeoclimate, such as sea-surface salinity, precipitation, shift in the Intertropical Convergence Zone (ITCZ) and the amplitude of the East Asian Monsoon (EAM), have also attracted increasing attention. Some authors have proposed that significant lower precipitation and/or higher salinity developed in the vicinity of the South China Sea during glacial periods (Wang, 1999; van der Kaars et al., 2001; De Deckker et al., 2002; Wang et al., 2003; Wei et al., 2003). On the other hand, Hu et al. (2003) pointed out that there was no obvious climate change from the last glacial period to the early Holocene in the southern South China Sea based on their *n*-alkanes data.

In this paper, we present in situ field evidence of dry climates during the late Cenozoic sea-level lowstands at the Nansha (Spratly) Islands, located near northwestern margin of the WPWP. Our evidence is derived from the occurrence of a climate-sensitive soil that developed on an islet, and is therefore independent of assumptions about ice volume and the original chemical composition of seawater.

When marine carbonates emerge during sea-level falls, either of two types of subaerial exposure surface (SES) may develop: a karst surface or a caliche surface (Esteban and Klappa, 1983). Caliche typically formed in sub-arid to sub-humid climate (Esteban and Klappa, 1983; James and Choquette, 1990; Milnes, 1992). Four caliche zones have been identified in the late Neogene sequence of Nansha and provide important palaeoclimate signatures, which may shed some new light on the palaeoclimate reconstruction of the tropical West Pacific.

2. Regional setting

The Nansha (Spratly) Islands of South China Sea consists of numerous atolls, reefs and banks. In the time span from 1995 to 2003, the annual rainfalls of Nansha Islands are in the range of 1800–2200 mm and the average temperature is 27 °C, ranging from 30 °C in summer to 25 °C in winter according to the Central Weather Bureau, Taiwan.

The tectonic history of the Nansha Islands has been dominated by crustal extension and rifting since the

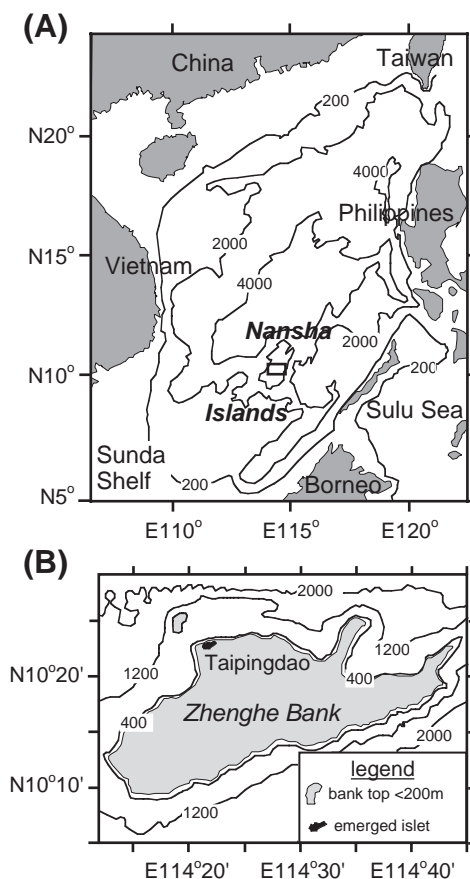


Fig. 1. (A) General geographic and bathymetric feature of the South China Sea. The rectangle in the center indicates the location of the Zhenghe Bank. (B) Simplified bathymetric feature of the Zhenghe Bank and location of Taipingdao. Based on the Hydrographic Data Bank System of South China Sea, Ministry of Transportation, ROC.

opening of the South China Sea in the Paleogene (Schulter et al., 1996). Block faulting ceased during the Middle to Late Miocene. Thermal subsidence has been the major tectonic component since then.

Taipingdao is the largest islet of Nansha Islands, and is located at 10°23'N and 114°22'E as part of the Zhenghe Bank (Fig. 1). It measures about 0.43 km² in area, covered by bioclastic sediments and guano deposits, and has a maximum elevation of 4 m.

3. Materials and methods

A fully cored borehole of 523.35 m in depth below the surface was drilled in 1981 at Taipingdao

by the Taiwanese Government and became accessible to us in recent years. The borehole is located in the southeastern Taipingdao at 2 m in elevation and all depths used in this paper are depths below the surface. The subsurface sequence can be divided into three sections in terms of mineralogy: 0–21 m aragonite and high-Mg calcite, 21–165.4 m low-Mg calcite, and below 165.4 m mostly dolomite. This paper focuses on the low-Mg calcite section because the palaeoclimatic signals are identified in this interval only. In total, 140 rock samples were collected from 21 to 165.4 m for petrographic and geochemical studies. The sampling interval ranged from about 0.5 m in well-recovered intervals to several meters in poorly recovered intervals. Thin sections and powder samples from matrix were prepared from the hand specimens.

Mineralogical identification was conducted using X-Ray Diffractometry. Stable carbon and oxygen isotope compositions were then analyzed using a Micro-mass IsoPrime mass spectrometer equipped with a multicarb automation system. Analyses were performed on about 0.1 mg of microsamples. CO₂ was evolved from the samples reacted with 100% phosphoric acid at 90 °C. Results are reported in the δ per mil notation with respect to the VPDB standard. Analytical calibration was monitored through repeated measurements of a NBS-19 standard. Analytical precision was better than $\pm 0.1\%$ ($N=108$) for both carbon, and oxygen isotopes. Elemental analyses of calcium and strontium were performed on an Elmer-Perkins 5100 PC Atomic Absorption Spectrophotometer and the regression coefficient of the standards was maintained at 0.9999 in all analyses.

4. Depositional sequence and stratigraphy

The lithological sequence of the Taipingdao borehole is summarized in Fig. 2. The lithofacies consists mainly of a reef facies that includes algal–coral boundstones and coral floatstones, and a lagoon facies that includes bioclastic wackestone/packstone and partially algal-banded bioclastic wackestone/packstone, while the diagenesis is dominated by meteoric diagenesis (Gong et al., 2003). Four pristine corals recovered in the interval of 9–12 m were dated by AMS C-14 to range from 4761 ± 115 to

4924 ± 104 yr BP. Another pristine coral recovered in the interval of 18–21 m was dated by AMS C-14 to be 7864 ± 87 yr BP (Fig. 2). The C-14 ages were calibrated using the CALIB Program v.5.0.1 developed by Stuiver and Reimer using the marine04 database and ΔR of South China Sea. Carbon and oxygen isotopes and the carbonate mineralogy suggest that the carbonates above 21 m have not been exposed to pervasive subaerial diagenesis. Therefore, the Holocene/Pleistocene boundary is placed at 21 m considering the AMS C-14 date and the Quaternary sea-level history (Chappel and Shackleton, 1986). Magnetostratigraphic studies reveal normal polarity from 26 to 43 m and reverse polarity from 43 to 45.5 m, below which the magnetic intensities become too weak to be identified (Fig. 2; Horng et al., unpublished data). The reversal at 43 m is interpreted to be the Brunhes/Matuyama boundary. Strontium isotope analysis showed that the $^{87}\text{Sr}/^{86}\text{Sr}$ ratios of the study section ranged from 0.70912 at 165.3 m to 0.70919 at 110.8 m and 0.70921 at 90.8 m (Fig. 2; You et al., in preparation). The study section is thus evidently Pleistocene in age (Farrel et al., 1995).

5. Occurrence of caliche

Caliches are weathering product or calcareous soil, developed on the surface of limestone or other rock types. They result from the dissolution of carbonate minerals and rapid reprecipitation of low-Mg calcite. Caliches that develop in non-carbonate rocks or alluvial gravels mostly occur in arid to semi-arid areas (Milnes, 1992; Lal et al., 2000). However, caliches developed on limestones usually occur in areas with higher precipitation, because the supply of calcium carbonate is sufficient and therefore a smaller evaporation–precipitation deficit is required. The typical condition for caliche development on limestone is a semi-arid climate but they can also occur in sub-humid areas if the climate is hot enough (Goudie, 1973; Esteban and Klappa, 1983).

Caliche profiles vary from place to place. Barbados at a latitude of 13°10'N may be the best analogue to Taipingdao. According to James (1972) and Harrison (1977), the thickness of Barbados caliche ranges from a few centimeters up to 2–3 m. There is usually a well

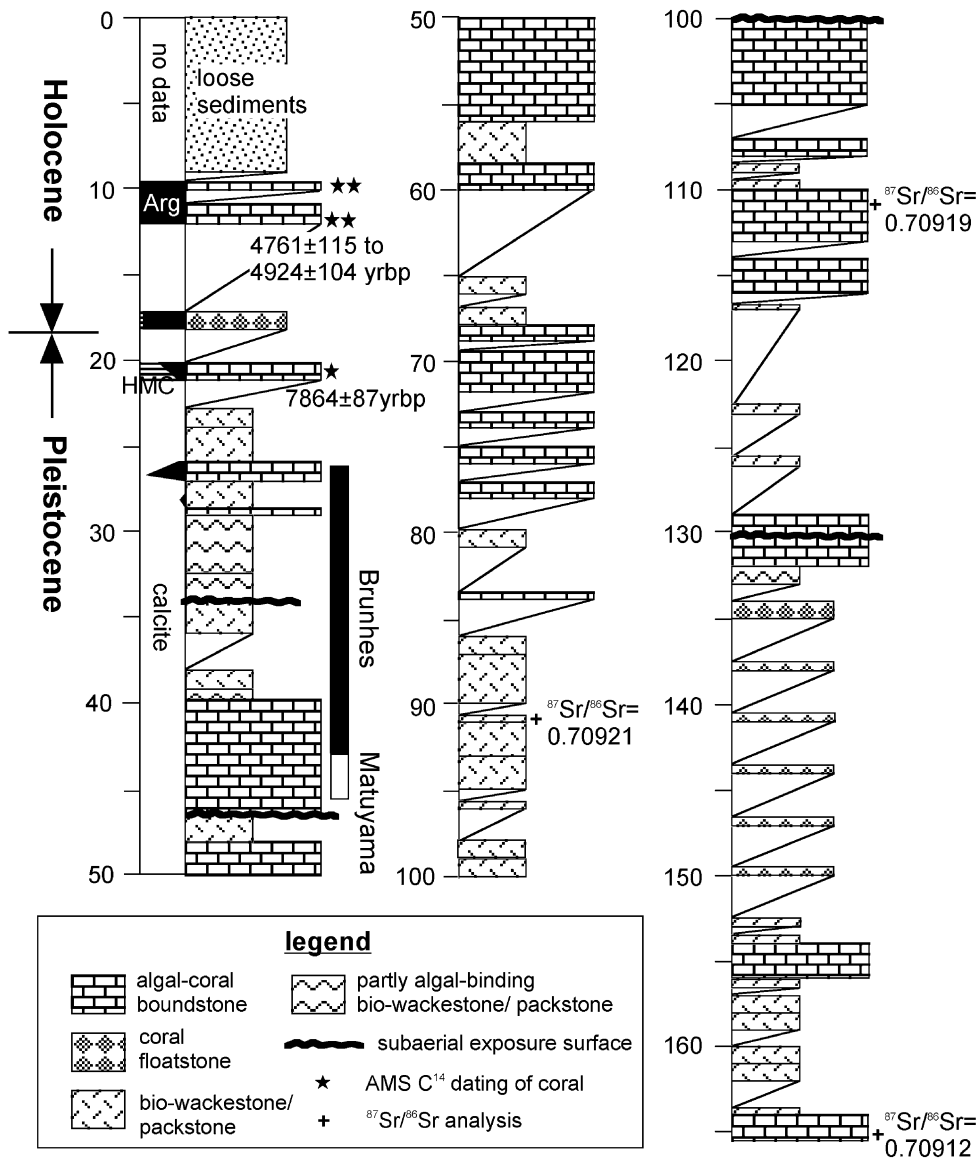


Fig. 2. Lithological column of 0~165.4 m of Taipingdao borehole. Note the transition from aragonite to calcite occur at 21 m, and the transition from calcite to dolomite occurs at 165.4 m. The asterisks signs mark the positions of pristine coral samples dated by AMS C-14 method. Ages are given next to the symbols.

indurated, gray to brown crust on top. The surficial crust is usually underlain by a zone of laminated, nodular or chalky carbonates. Between the caliche and the underlying host limestone, there may be a brecciated transition zone in which the caliche develops in fractures while the host limestone remains unaltered.

6. Petrography of the Nansha caliche

Dissolution cavities, mineral stabilization, and porosity-rimming and/or drusy cementation of low-Mg calcite were extensively found in the samples. Four subaerial diagenetic zones are identified at 34.2~36, 46.7~47.3, 100~105 and 129.4~132 m respectively

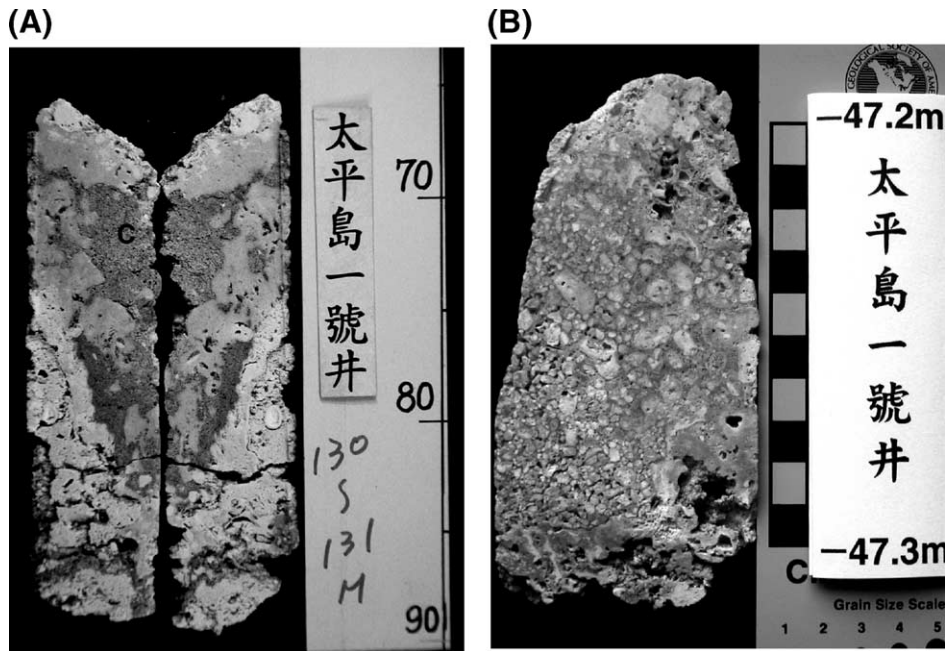


Fig. 3. Photographs of Taipingdao core sample. (A) Corroded limestone nodules embedded in reddish matrix at 47.3 m. The scale is in the photograph. (B) Caliche (C) developed in fractures of the host limestone at 130.9 m. The vertical scale is in centimeters.

(Fig. 2). Alveolar texture, micro-rhizolith (plant-root structure) and caliche glaebules were observed in all four zones (Figs. 3 and 4). Corroded limestone nodules embedded in reddish matrix and meniscus cement were also observed at 46.7–47.3 m. The laminated crust and chalky, massive layer that commonly developed in caliche were not preserved in Taiping-

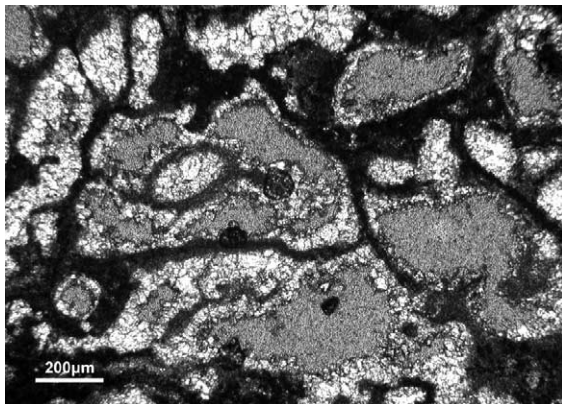


Fig. 4. Photomicrograph of the alveolar structure and micro-rhizolith observed at 47.3 m. The scale is on the photomicrograph. Under transmitted light.

dao; presumably being eroded away during sea-level rises. Instead, mottled caliches with alveolar texture developed in host-rock fractures are best represented (Fig. 3).

Several features are considered to be diagnostic of a caliche, among which rhizoliths, alveolar structure and caliche glaebules are considered to be the major ones (Esteban and Klappa, 1983). Floating structure (corroded limestone clasts in silt-sized, reddish matrix) is also characteristic, although not diagnostic, of a caliche. All of these features were observed at Taipingdao. We therefore interpret these SES to be caliche in origin.

7. Geochemical analysis

The results of isotopic analyses are plotted in Fig. 5. Isotopic compositions of the low-Mg calcite samples exhibit a wide range in $\delta^{13}\text{C}$ composition from -1.15‰ to -10.06‰ and a relative narrower range in $\delta^{18}\text{O}$ composition from -4.44‰ to -8.68‰ . Both are typical of meteoric diagenesis (James and Choquette, 1990; Morse and Mackenzie, 1990).

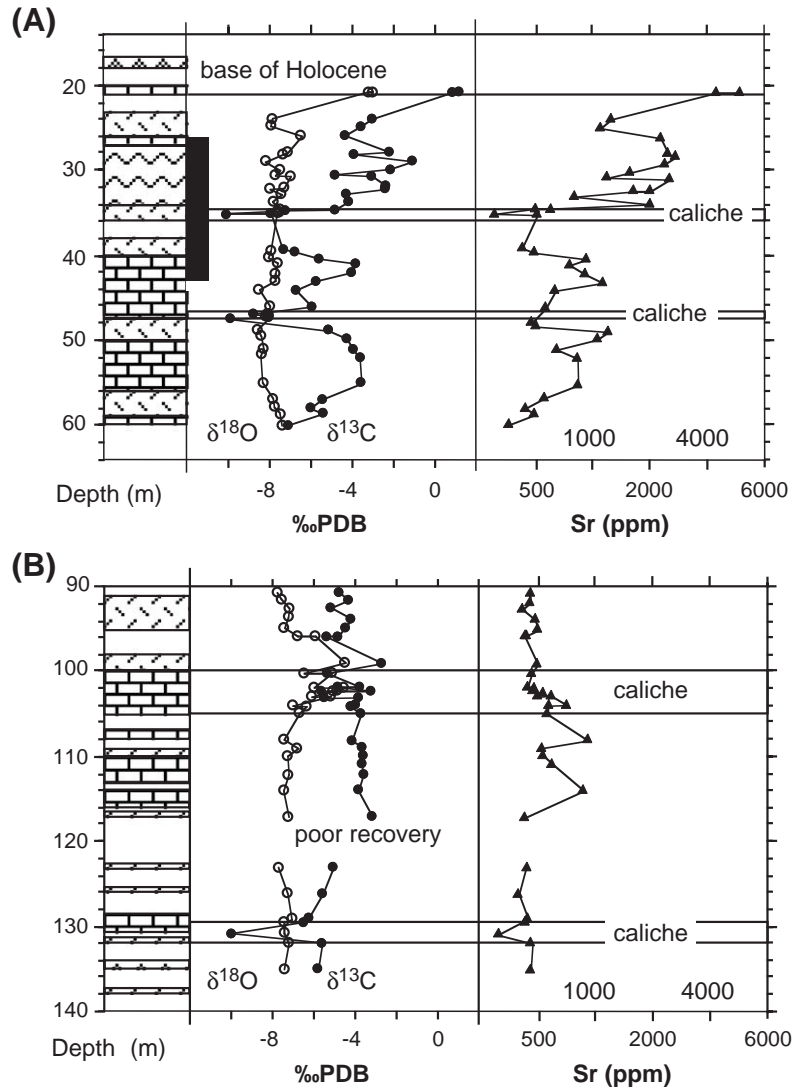


Fig. 5. Diagenetic stratigraphy of the Taipingdao borehole. Note the depletion in isotopic and strontium compositions in the caliche zones. The scale of Sr concentration is not linear. See Fig. 2 for the legend of lithology. (A) The upper two caliche layers. Note the uppermost two samples are aragonite, while the others are low-Mg calcite. (B) The lower two caliche layers. All samples consist of low-Mg calcite.

Upward depletion in $\delta^{13}\text{C}$ is observed at the four SES (Fig. 5). $\delta^{18}\text{O}$ values also show upward depletion at 34, 47 and 130 m, but become enriched in the interval of 100–105 m. Strontium elemental compositions also show an upward depletion toward the top of each SES. $\delta^{18}\text{O}$ mostly show parallel trends to those of $\delta^{13}\text{C}$ but display upward enrichment at 100 m.

Stratigraphic profiles of $\delta^{13}\text{C}$, $\delta^{18}\text{O}$ and Sr compositions in the meteoric diagenetic zones

have been well established in many Pleistocene carbonate sequences (James and Choquette, 1990; Morse and Mackenzie, 1990). Upward depletion in $\delta^{13}\text{C}$ is characteristic of a meteoric vadose environment because of exchange with lighter carbon from soil gas (James and Choquette, 1990). When marine aragonite is converted to calcite in meteoric environment, Sr concentrations in the carbonates are also drastically reduced, and are mostly deplet-

ed at top of the vadose zone (Brand and Veiser, 1980).

Stratigraphic variations in $\delta^{18}\text{O}$ usually are parallel to those of $\delta^{13}\text{C}$ but may show enrichment at the very top of the vadose zone (James and Choquette, 1990; Morse and Mackenzie, 1990). Such enrichment of $\delta^{18}\text{O}$ is caused by water evaporation. The continuous $\delta^{18}\text{O}$ increase in 105–100 m in the Taipingdao column is unusual and may indicate an extended period of subaerial exposure under an evaporation-dominant climate (Fig. 5B).

8. Discussion

8.1. Subaerial exposure and eustasy

Petrographic and geochemical data revealed at least four SES in the pre-Holocene section. An SES develops when carbonate sediments become emerged by eustatic sea-level falls or land uplift. Regional studies in the South China Sea suggest that the tectonic activity of Nansha Islands ceased after the middle to late Miocene (Schulter et al., 1996). The late Neogene tectonic history of the study area is thus dominated by thermal subsidence. On the other hand, two types of eustatic sea-level fluctuations in late Cenozoic are well documented: glacioeustasy and third-order eustatic sea-level changes. Multiple SES caused by Quaternary glacioeustatic sea-level falls have been identified in several drilling sites in banks and atolls (Boardman et al., 1986; Quinn, 1991; Melim, 1996; among others). On the other hand, sequence stratigraphy has also identified third-order sea-level lowstands at 0.8, 1.6, 2.4 and 3.0 Ma (Haq et al., 1988). Although we cannot correlate each SES to a specific sea-level fall nor determine the order of these eustatic changes, it is evident that these caliches were developed during eustatic sea-level lowstands when the extend of the South China Sea was greatly reduced.

8.2. The caliche and its palaeoclimatic implications

Late Pleistocene or Holocene caliches that developed on limestones have mostly been found in semi-arid areas (Goudie, 1973; Watts, 1980; Coniglio and

Harrison, 1983; Esteban and Klappa, 1983; among others). However, caliche was formed in coastal plain of Barbados where the annual precipitation is about 1100–1250 mm (Harrison, 1977). The latitude and island setting of Barbados are similar to those of Nansha, thus Barbados can serve as a better analogue than other cases. The Nansha area might have experienced sub-arid to sub-humid climate with annual precipitation no more than 1200 mm in the past, compared with the 1800–2200 mm of modern annual precipitation.

The reduced precipitation and presumably enhanced evaporation would result in substantial decrease of the meteoric component in the surface seawater, and consequently higher salinities and heavier $\delta^{18}\text{O}$ compositions (De Deckker et al., 2002). This factor should be taken into consideration by palaeoclimate modelers.

Furthermore, foraminiferal $\delta^{18}\text{O}$ records from the South China Sea exhibit much greater amplitudes during glacial–interglacial fluctuation compared with those of the Sulu Sea (Wei et al., 2003). Other evidences of a dry climate or a reduced WPWP during glacial periods have also been reported, such as pollen records on land in Southeast Asia and North Australia (Torgersen et al., 1988; van der Kaars and Dam, 1995; van der Kaars et al., 2001). We believe that the Nansha caliches can serve as direct evidence for a dry climate in the central South China Sea during sea-level lowstands prior to the Last Glacial Maximum. Such a dry climate in a tropical sea can be best explained by a southward shift of ITCZ, a reduced strength of EAM and a reduced size of WPWP during glacial periods.

9. Conclusions

At least four caliche zones have been identified in the subsurface carbonates of Nansha Islands and are interpreted to develop during eustatic sea-level lowstands. Strontium isotope and magnetostratigraphic studies showed that the caliches are Pleistocene in age although we are unable to correlate each caliche layer to a specific sea-level lowstand.

Caliche typically occurs in sub-arid to sub-humid areas when developed on limestones. The occurrence of these four caliche zones strongly indicates that the

central South China Sea experienced episodes of significantly drier climate during Pleistocene sea-level lowstands than the present. This conclusion is consistent to earlier studies based on different approaches (van der Kaars et al., 2001; De Deckker et al., 2002). However, the Taipingdao caliches are in situ evidence of palaeoclimate and independent of assumptions of or ice volume or chemical composition of seawater.

Acknowledgements

We thank the Chinese Petroleum Corp. (CPC), Taipei for providing the research materials. We thank Wu-Bin Su of CPC, Kun-Wei Chung, Chien-Hui Hong and Shu-Chuan Chen of the National Museum of Natural Science, Taichung for their laboratory assistance. Dr. De Deckker and three anonymous reviewers provided valuable comments on an early version of the manuscript. This study was supported by the National Science Council, Republic of China under the grants NSC 87-2116-M-178-001 and NSC 88-2116-M-178-001.

References

- Boardman, M.R., Neumann, A.C., Baker, P.A., Dulin, L.A., Kenter, R.J., Hunter, G.E., Kiefer, K.B., 1986. Banktop responses to Quaternary fluctuations in sea level recorded in periplatform sediments. *Geology* 14, 28–31.
- Brand, U., Veiser, J., 1980. Chemical diagenesis of a multicomponent carbonate system-1: trace elements. *J. Sediment. Petrol.* 50, 1219–1236.
- Chappel, J., Shackleton, N.J., 1986. Oxygen isotopes and sea-level. *Nature* 324, 137–140.
- Coniglio, M., Harrison, R., 1983. Holocene and Pleistocene caliche from Big Pine Key, Florida. *Bull. Can. Pet. Geol.* 31, 3–13.
- De Deckker, P., Tapper, N.J., van der Kaars, S., 2002. The status of the Indo-Pacific Warm Pool and adjacent land at the Last Glacial Maximum. *Glob. Planet. Change* 35, 25–35.
- Esteban, M., Klappa, C.F., 1983. Subaerial exposure environment. In: Scholle, P.A., Bebout, D.G., Moore, C.H. (Eds.), *Carbonate Depositional Environments*, Amer. Assoc. Petrol. Geol. Mem., vol. 33, pp. 1–72.
- Farrel, J.W., Clemens, S., Gromet, L.P., 1995. Improved chronostratigraphic reference curve of Late Neogene sea-water $^{87}\text{Sr}/^{86}\text{Sr}$. *Geology* 23, 403–406.
- Gong, S.-Y., Mii, H.-S., Yui, T.-F., Huang, F.-W., Torng, P.-K., Chi, W.-R., Huang, S.-T., Wang, S.-W., Yang, K.-M., Wu, J.-C., 2003. Deposition and diagenesis of late Cenozoic carbonates in Nansha (Spratly) Islands, South China Sea. *West. Pac. Earth Sci.* 3, 93–106.
- Goudie, A., 1973. *Duricrusts in Tropical and Subtropical Landscapes*. Clarendon, Oxford. 184 pp.
- Haq, B.U., Hardenbol, J., Vail, P., 1988. Mesozoic and Cenozoic chronostratigraphy and eustatic cycles. In: Wilgus, C.K., Hastings, B.S., Kendall, C.G.St.C., Posamentier, H.W., Ross, C.A., van Wagoner, J.C. (Eds.), *Sea-level Changes: An Integrated Approach*, 42. SEPM Spec. Publ., pp. 71–108.
- Harrison, R.S., 1977. Caliche profiles: indicators of near-surface subaerial diagenesis, Barbados, West Indies. *Bull. Can. Pet. Geol.* 25, 123–173.
- Hu, J., Peng, P., Fang, D., Jia, G., Jian, Z., Wang, P., 2003. No aridity in Sunda Land during the last glaciation: evidence from molecular-isotope stratigraphy of long-chain *n*-alkanes. *Palaeogeogr. Palaeoclimatol. Palaeoecol.* 201, 269–281.
- James, N.P., 1972. Holocene and Pleistocene calcareous crust (caliche) profiles: criteria for subaerial exposure. *J. Sediment. Petrol.* 42, 817–836.
- James, N.P., Choquette, P.W., 1990. Limestones—the meteoric diagenetic environment. In: McIlreath, I.A., Morrow, W. (Eds.), *Diagenesis*. Geosci. Can, reprint series, vol. 4, pp. 35–73.
- Lal, R., Kimble, J.M., Eswaran, H., Stewart, B.A., 2000. *Global Climatic Change and Pedogenic Carbonates*. CRC Press, Boca Raton. 305 pp.
- Lea, D.W., Martin, P.A., Dorothy, K.P., Spero, H.J., 2002. Reconstructing a 350 ky history of sea level using planktonic Mg/Ca and oxygen isotope records from a Cocos Ridge core. *Quat. Sci. Rev.* 21, 283–293.
- Melim, L.A., 1996. Limitations on lowstand meteoric diagenesis in the Plio-Pleistocene of Florida and Great Bahamas Bank: implications for eustatic sea-level models. *Geology* 24, 893–896.
- Milnes, A.R., 1992. Calcrete. In: Martini, I.P., Chesworth, W. (Eds.), *Weathering, Soils, and Paleosols*. Elsevier, Amsterdam, pp. 309–347.
- Morse, J.W., Mackenzie, F.T., 1990. *Geochemistry of Sedimentary Carbonates*. Elsevier, New York. 707 pp.
- Quinn, T.M., 1991. Meteoric diagenesis of Plio-Pleistocene limestones at Enewetak Atoll. *J. Sediment. Res.* 61, 681–703.
- Schulter, H.U., Hinz, K., Block, M., 1996. Tectono-stratigraphic terranes and detachment faulting of the South China Sea and Sulu Sea. *Mar. Geol.* 130, 39–78.
- Torgersen, T., Luly, J., De Deckker, P., Jones, M.R., Sealer, D.E., Chivas, A.R., Ullman, W.J., 1988. Late Quaternary environments of the Carpentaria Basin, Australia. *Palaeogeogr. Palaeoclimatol. Palaeoecol.* 67, 245–261.
- van der Kaars, W.A., Dam, M.A.C., 1995. A 135,000-year record of vegetational and climatic change from the Bandung area, West-Java Indonesia. *Palaeogeogr. Palaeoclimatol. Palaeoecol.* 117, 55–72.
- van der Kaars, S., Penny, D., Tibby, J., Fluin, J., Dam, R., Suparan, P., 2001. Late Quaternary palaeoecology, palynology, and palaeolimnology of a tropical lowland swamp: Rawa Danau, West Java, Indonesia. *Palaeogeogr. Palaeoclimatol. Palaeoecol.* 171, 185–212.

- Watts, N.L., 1980. Quaternary pedogenic calcretes from the Kalahari (southern Africa): mineralogy, genesis and diagenesis. *Sedimentology* 27, 661–686.
- Wang, P., 1999. Response of western Pacific marginal seas to glacial cycles. Paleooceanographic and sedimentological features. *Mar. Geol.* 156, 5–39.
- Wang, P., Jian, Z., Zhao, Q., Li, Q., Wang, R., Liu, Z., Wu, G., Shao, L., Wang, J., Huang, B., Fang, D., Tian, J., Li, J., Li, X., Wei, G., Sun, X., Luo, Y., Su, X., Mao, S., Chen, M., 2003. Evolution of the South China Sea and monsoon history revealed in deep-sea records. *Chin. Sci. Bull.* 156, 5–39.
- Wei, K.-Y., Chiu, T.-C., Chen, Y.-G., 2003. Toward establishing a maritime proxy record of the East Asian summer monsoons for the late Quaternary. *Mar. Geol.* 201, 67–79.
- You, C.-F., Ho, K.-S., Wang, S.-W., Li, M.-D., in preparation, The systematic evolution of $^{87}\text{Sr}/^{86}\text{Sr}$ ages in marine carbonates on land Taiwan: tectonic implication. to be submitted to *Chem. Geol.*